

BILLWISEITE, IDEALLY $\text{Sb}^{3+}5(\text{Nb},\text{Ta})_3\text{WO}_{18}$, A NEW OXIDE MINERAL SPECIES FROM THE STAK NALA PEGMATITE, NANGA PARBAT – HARAMOSH MASSIF, PAKISTAN: DESCRIPTION AND CRYSTAL STRUCTURE

FRANK C. HAWTHORNE[§], MARK A. COOPER, NEIL A. BALL, YASSIR A. ABDU AND PETR ČERNÝ

Department of Geological Sciences, University of Manitoba, Winnipeg, Manitoba R3T 2N2, Canada

FERNANDO CÁMARA

*Dipartimento di Scienze della Terra, Università di degli Studi di Torino,
 via Valperga Caluso 35, I-10125 Torino, Italy*

BRENDAN M. LAURS

Gemological Institute of America, 5345 Armada Drive, Carlsbad, California 92008, USA

ABSTRACT

Billwiseite, ideally $\text{Sb}^{3+}5(\text{Nb},\text{Ta})_3\text{WO}_{18}$, is an oxide mineral from a granitic pegmatite on the eastern margin of the Nanga Parbat – Haramosh massif at Stak Nala, 70 km east of Gilgit, Pakistan. It is transparent, pale yellow (with a tinge of green), has a colorless to very pale-yellow streak, a vitreous luster, and is inert to ultraviolet radiation. Crystals are euhedral with a maximum size of $\sim 0.5 \times 0.25 \times 0.15$ mm and show the following forms: $\{100\}$ pinacoid $\approx \{011\}$ pinacoid $\approx \{410\}$ prism; contact twins on $\{100\}$ are common. Cleavage is $\{100\}$ indistinct. Mohs hardness is 5, and billwiseite is brittle with a hackly fracture. The calculated density is 6.330 g/cm³. The indices of refraction were not measured; the calculated index of refraction is 2.3, $2V(obs) = 76(2)^\circ$. Billwiseite is colorless in transmitted light, non-pleochroic, and the optic orientation is as follows: $X \parallel \mathbf{b}$, $Y \wedge \mathbf{c} = 72.8^\circ$ (in β acute). It occurs scattered across the surface of a large ($\sim 5 \times 2.5 \times 1.3$ cm) crystal of lepidolite from a miarolitic cavity. The most abundant minerals in the cavities at Stak Nala are albite, quartz, K-feldspar, tourmaline, muscovite or lepidolite, topaz and fluorite, and billwiseite can be partly mantled by B-rich muscovite. Billwiseite is monoclinic, space group $C2/c$, a 54.116(5), c 5.5482(5) Å, β 90.425(2)°, V 1475.5(2) Å³, $Z = 4$, $a:b:c = 11.012 : 1 : 1.131$. The strongest seven lines in the X-ray powder-diffraction pattern [d in Å(l) hkl] are as follows: 3.147(100)(91 $\bar{1}$, 911), 3.500(55) (51 $\bar{1}$, 511), 1.662(53)(142 $\bar{2}$), 3.017(48)(1800), 1.906(47)(1820), 1.735(30)(113, 113), 1.762(25)(271 $\bar{1}$, 2711). Chemical analysis by electron microprobe gave Nb_2O_5 12.03, Ta_2O_5 19.31, Sb_2O_3 48.34, TiO_2 0.99, WO_3 19.96, sum 100.63 wt.% where the valence state of Sb was determined by crystal-structure analysis. The resulting empirical formula on the basis of 18 O anions is $\text{Sb}^{3+}4.87(\text{Nb}_{1.33}\text{Ta}_{1.28}\text{Ti}_{0.18}\text{W}_{1.26})\Sigma 4.05\text{O}_{18}$. The crystal structure of billwiseite was solved by direct methods and refined to an R_1 index of 4.71% based on 2122 observed reflections collected on a three-circle diffractometer with $\text{MoK}\alpha$ X-radiation. The structure consists of two distinct sheets of M (= Ta, Nb, W) octahedra and three distinct sheets of Sb^{3+} polyhedra parallel to (100) . These sheets alternate in the \mathbf{a} direction to form a continuous structure.

Keywords: billwiseite, new mineral species, oxide, crystal structure, electron-microprobe analysis, optical properties, X-ray powder-diffraction pattern, granitic pegmatite, Nanga Parbat – Haramosh massif, Stak Nala, Gilgit, Pakistan.

INTRODUCTION

The granitic pegmatites at Stak Nala, Karakoram Mountains, northern Pakistan, belong to the LCT (Li–Cs–Ta) family, with characteristics transitional between the elbaite and lepidolite subtypes, and overtones of the miarolitic (Mi–Li) subclass (Černý & Ercit 2005). Multicolored elbaite has been mined from miarolitic

cavities in the pegmatites since the early 1980s. Most of the production of tourmaline and associated minerals has come from a single 1-m-thick sill within a swarm of at least six flat-lying subparallel sills that are nearly concordant to the foliation of the enclosing gneisses. During mapping and detailed characterization of the pegmatite (Laurs *et al.* 1998), an unknown mineral was discovered and subsequently characterized as a

[§] E-mail address: frank_hawthorne@umanitoba.ca

new species: billwiseite. Billwiseite is named after William Stewart Wise, Professor of Geology Emeritus, University of California at Santa Barbara. Bill was born on August 18, 1933, in Carson City, Nevada, and holds degrees from Stanford University and Johns Hopkins University. During his career at UCSB, he published many papers in mineralogy and igneous petrology, and described several new minerals in the zeolite, arsenate, and vanadate groups. The name recognizes his contributions to mineralogy and his inspiration and mentoring of mineralogy students at UCSB.

The new mineral and mineral name have been approved by the Commission on New Minerals, Nomenclature and Classification, International Mineralogical Association (IMA 2010-053). The holotype specimen of billwiseite has been deposited in the mineral collection of the Royal Ontario Museum, catalogue number M55951.

OCCURRENCE

The granitic pegmatites at Stak Nala, Karakoram Mountains, northern Pakistan, are located 70 km east of Gilgit, and 13 km north of the Indus River, on the west side of the Stak valley at an elevation of approximately 2800 m a.s.l., $35^{\circ}44'37''\text{N}$, $75^{\circ}02'35''\text{E}$. A rough dirt road leads from the Gilgit–Skardu road to Toghla village, and a footpath accesses the pegmatites about 2 km north and 400 m above the valley floor. They lie within the eastern margin of the Nanga Parbat–Haramosh Massif, which forms the northernmost exposure of Indian Plate rocks; the massif has been rapidly uplifted and exhumed during the past 10 Ma through the overlying rocks of the Kohistan–Ladakh arc terrane. The host rocks of the pegmatite consist of paragneiss and orthogneiss that probably correlate with the Shengus gneiss of Madin (1986). The gneisses are recrystallized to a granoblastic texture and have a mineral assemblage of quartz, K-feldspar, plagioclase, biotite and garnet, characteristic of the upper amphibolite to granulite facies.

The pegmatites form sill-like bodies that typically range from 0.3 to 1.2 m thick and 30 m to at least 120 m long, and show symmetrical textural and mineralogical zoning (with no footwall aplite) parallel to contacts: a coarse-grained border zone grades into a very coarse-grained wall zone that surrounds a locally continuous core that is dominated by blocky K-feldspar. The core zone contains sporadic crystal-lined cavities or “pockets”. Replacement by albite is widespread, particularly in areas containing abundant pocket mineralization. The most abundant pocket minerals are albite, quartz, K-feldspar, tourmaline, muscovite or lepidolite, topaz and fluorite, which form euhedral crystals that project into the cavities from the surrounding pegmatite and also form broken crystals that litter the floor of the pockets. Partially coating all minerals in most pockets is an aggregate of fine-grained muscovite or B-rich

muscovite (up to 3.8 wt% B_2O_3) that forms a hard granular to porcelaneous layer typically <1 mm thick.

Billwiseite was found on a single specimen of lepidolite recovered from the mine dump and is inferred to have formed in a pegmatite pocket. The lepidolite consists of a large (5.4 cm), colorless, euhedral crystal that is partly coated by a druse of billwiseite and B-rich muscovite that completely covers the billwiseite on one part of the specimen, but is absent elsewhere (Fig. 1). Billwiseite is intergrown with and overgrown by B-rich muscovite, suggesting that it formed slightly before and during crystallization of the B-rich muscovite.

PHYSICAL PROPERTIES

Billwiseite forms pale yellow (with a suggestion of green) blocky crystals scattered across the surface of a large ($5.4 \times 2.5 \times 1.3$ cm) crystal of lepidolite. Individual crystals of billwiseite are euhedral (Fig. 1) with a maximum size of $\sim 0.5 \times 0.25 \times 0.15$ mm, and show the following forms (Fig. 2): $\{100\}$, $\{011\}$, $\{410\}$. Contact twins on $\{100\}$ are common, and $a:b:c$ are in the proportion 11.0258 : 1 : 1.1297 (based on cell dimensions).

Billwiseite is transparent, pale yellow (with a tinge of green) and has a colorless to very pale yellow streak, a vitreous luster, and is inert to ultraviolet radiation. The cleavage is $\{100\}$ indistinct, and the Mohs hardness is 5. Billwiseite is brittle with a hackly fracture. The calculated density is 6.330 g/cm^3 . The indices of refraction were not measured; the calculated index of refraction is 2.3, and the $2V(\text{obs.})$ is $76(2)^\circ$. Billwiseite is colorless in transmitted light, non-pleochroic, and the optic orientation is as follows: $X \parallel \mathbf{b}$, $Y \wedge \mathbf{c} = 72.8^\circ$ (in β acute).

CHEMICAL COMPOSITION

Crystals were analyzed with a Cameca SX-100 electron microprobe operating in wavelength-dispersion mode with an accelerating voltage of 15 kV, a specimen current of 20 nA, and a beam diameter of 5 μm . The following standards were used: Nb: $\text{Ba}_2\text{NaNb}_5\text{O}_{15}$; Ta: $\text{MnNb}_2\text{Ta}_2\text{O}_9$; Sb: stibiotantalite; Ti: titanite; W: CaWO_4 . The data were reduced and corrected by the PAP method of Pouchou & Pichoir (1985). The absence of (OH) and (H_2O) groups was established by crystal-structure solution and refinement, and further confirmed by infrared spectroscopy. Table 1 gives the chemical composition (mean of eight determinations) and the chemical formula based on 18 anions per formula unit (pfu). The empirical formula is as follows: $\text{Sb}^{3+}_{4.87}(\text{Nb}_{1.33}\text{Ta}_{1.28}\text{Ti}_{0.18}\text{W}_{1.26})\Sigma_{4.05}\text{O}_{18}$. Assuming that the Sb sites are completely occupied by Sb^{3+} , Ti must enter the structure via the substitution $\text{Ti} + \text{W} \rightarrow (\text{Nb}, \text{Ta})_2$. We may write the ideal formula as $\text{Sb}^{3+}_{5}(\text{Nb}, \text{Ta})_3\text{WO}_{18}$. Although W is disordered with Nb and Ta at the $M(1)$ and $M(2)$ sites in the structure, its amount is fixed by

TABLE 1. CHEMICAL COMPOSITION AND CHEMICAL FORMULA OF BILLWISEITE

	wt. %	Range	Stand. dev.	Cation	apfu
Nb ₂ O ₅	12.03	10.33 - 15.05	1.38	Nb	1.33
Ta ₂ O ₅	19.31	13.93 - 20.44	2.42	Ta	1.28
Sb ₂ O ₃	48.34	47.99 - 48.52	0.42	Ti	0.18
TiO ₂	0.99	0.81 - 1.01	0.03	W	1.26
WO ₃	19.96	19.06 - 22.42	1.34	Sum	4.05
Total	100.63	99.50 - 101.31	0.75	Sb	4.87

electroneutrality at 1 *apfu* in the absence of Ti. There is significant variation in the Nb and Ta contents: $1.7 \geq \text{Nb} \geq 1.2$ and $1.4 \geq \text{Ta} \geq 0.9$ *apfu* within single crystals. At extreme compositions, Ta does exceed Nb ($\sim \text{Ta}_{1.4}\text{Nb}_{1.2}$), but this is generally not the case: the values are close, with Nb generally being dominant (see Table 1). Because of the rarity of billwiseite and the fact that compositions tend to cluster around Nb slightly more than Ta, we propose billwiseite as a single species with Nb dominant and an end-member formula $\text{Sb}^{3+}_5\text{Nb}_3\text{WO}_{18}$.

X-RAY POWDER DIFFRACTION

The powder-diffraction pattern was recorded with graphite-monochromated $\text{CuK}\alpha$ X-radiation ($\lambda = 1.54178 \text{ \AA}$) on a Bruker D8 Discover SuperSpeed micro-powder diffractometer with a multi-wire 2D (Hi-Star) detector using a smear mount on a zero-background quartz plate and no internal standard. Table 2 shows the X-ray powder-diffraction data for billwiseite. The unit-cell parameters were refined by least-squares, giving the following values: $a = 54.19(4)$, $b = 4.929(3)$, $c = 5.557(3) \text{ \AA}$, $\beta = 90.17(5)^\circ$, $V = 1484.4(1.1) \text{ \AA}^3$.

INFRARED SPECTROSCOPY

The infrared spectrum (Fig. 3) shows relatively sharp bands at 710, 630, and 530 cm^{-1} due to coupled modes of the $(\text{Nb}, \text{Ta}, \text{Ti}, \text{W})\text{O}_6$ octahedra and SbO_n polyhedra, and a broad featureless region between ~ 1000 and 4000 cm^{-1} that is in accord with the absence of (OH) and (H_2O).

CRYSTAL-STRUCTURE SOLUTION AND REFINEMENT

A crystal was attached to a glass fiber and mounted on a Bruker-AXS diffractometer, equipped with a SMART Apex CCD detector and $\text{MoK}\alpha$ X-radiation. A total of 11046 reflections was measured out to 60° 2θ with a frame width of 0.2° ω and a frame time of 5 s. Unit-cell dimensions were determined from 5795 reflections with $|\text{F}| > 10\sigma\text{F}$, and are given in Table 3, together with other information pertaining to data collection and structure refinement. Of the 2138

TABLE 2. X-RAY POWDER-DIFFRACTION PATTERN OF BILLWISEITE

<i>I</i> _{obs}	<i>I</i> _{calc}	<i>d</i> _{obs}	<i>d</i> _{calc}	<i>h</i>	<i>k</i>	<i>l</i>	<i>I</i> _{obs}	<i>I</i> _{calc}	<i>d</i> _{obs}	<i>d</i> _{calc}	<i>h</i>	<i>k</i>	<i>l</i>	
1	14	5.418	5.417	10	0	0	6	3	1.946	1.948	14	2	1	
5	13	4.497	4.486	5	1	0	1				1.942	20	0	2
55	26	3.500	3.492	5	1	1	47	25	1.906	1.906	18	2	0	
"	40	"	3.488	5	1	1	9	10	1.843	1.845	22	0	2	
100	82	3.154	3.147	9	1	1	"	3	"	1.843	0	2	2	
"	84	"	3.141	9	1	1	30	11	1.828	1.827	4	2	2	
48	100	3.017	3.009	18	0	0	"	10	"	1.826	4	2	2	
18	15	2.770	2.779	0	0	2	1	1	1.806	1.807	6	2	2	
"	15	"	2.764	13	1	1	25	14	1.762	1.764	27	1	1	
18	31	2.730	2.723	4	0	2	"	17	"	1.761	27	1	1	
"	24	"	2.720	4	0	2	30	6	1.735	1.733	1	1	3	
3	26	2.570	2.573	8	0	2	"	4	"	1.733	1	1	3	
23	35	2.462	2.464	0	2	0	13	5	1.714	1.713	5	1	3	
9	2	2.248	2.247	9	1	2	"	7	"	1.711	5	1	3	
"	11	"	2.254	14	0	2	53	8	1.662	1.665	14	2	2	
4	2	2.219	2.222	4	2	1	4	3	1.626	1.624	5	3	0	
"	2	"	2.222	4	2	1	8	5	1.599	1.602	13	1	3	
2	0.5	2.126	2.125	23	1	0	"	4	"	1.599	13	1	3	
2	1	2.083	2.091	13	1	2	8	3	1.571	1.580	31	1	1	
3	6	2.048	2.044	18	0	2	"	1	"	1.578	31	1	1	
3	10	2.037	2.039	18	0	2	"	1	"	1.573	18	2	2	
8	5	1.989	1.986	23	1	1	10	2	1.560	1.571	18	2	2	

Values of *d* are quoted in \AA .

TABLE 3. MISCELLANEOUS REFINEMENT DATA FOR BILLWISEITE

Unit-cell parameters	<i>a</i> , <i>b</i> , <i>c</i> (\AA)	54.116(5), 4.9143(5), 5.5482(5)
	β (°)	90.425(2)
	<i>V</i> (\AA^3)	1475.5(2)
Space group		<i>C</i> 2/c
<i>Z</i>		4
<i>D</i> _{calc} (g/cm ³)		6.330
Radiation, filter		MoK α , graphite
2θ range for data collection (°)		1.50-60.00
<i>R</i> (int) (%)		5.64
Reflections collected		11046
Independent reflections		2138
Reflections with <i>F</i> > 4σ <i>F</i>		2122
Refinement method		Full-matrix least squares on <i>F</i> ² , fixed weights proportional to 1/σ <i>F</i>
Final <i>R</i> (<i>F</i> _{obs}) (%) [<i>F</i> > 4σ <i>F</i>]		<i>R</i> ₁ = 4.71
<i>R</i> indices (all data) (%)		<i>R</i> ₂ = 4.77, <i>wR</i> ₂ = 10.26, <i>GooF</i> = 1.186

unique reflections, 2122 reflections were considered as observed [$|F| > 4\sigma F$]. Absorption corrections were done using the program SADABS (Sheldrick 2008). The data were then corrected for Lorentz, polarization and background effects, averaged and reduced to structure factors.

All calculations were done with the SHELXTL PC (Plus) system of programs; *R* indices are given in Table 3 and are expressed as percentages. Systematic absences in the single-crystal X-ray diffraction data are consistent with monoclinic symmetry, space group *C*2/c. The structure was solved in this space group by direct methods and refined by full-matrix least-squares to an *R*₁ index of 4.71%. The *M*(1) and *M*(2) sites are



FIG. 1. Billwiseite (shiny yellow euhedral crystals) and B-rich muscovite (whitish grey) on the surface of a crystal of lepidolite. The field of view is 1.22 mm. Figure 1 was provided by Nathan Renfro/GIA. (GIA = Gemological Institute of America).

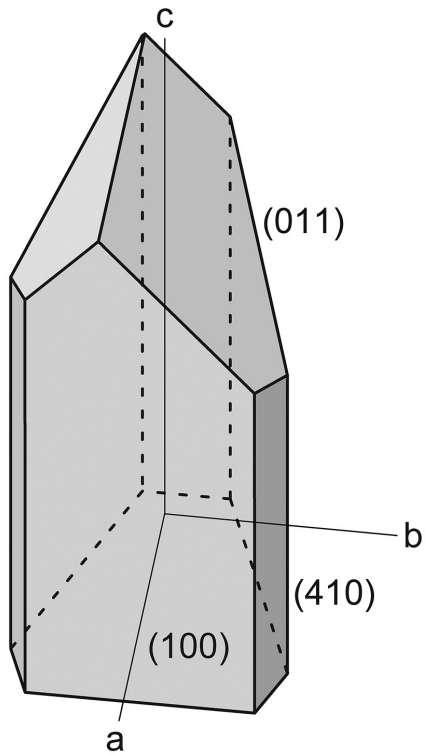


FIG. 2. Clinographic projection of a crystal of billwiseite, showing the morphology.

occupied by Nb, Ta, W and Ti. As the site-scattering refinement (Hawthorne *et al.* 1995) can only give information on two scattering species at a site (Hawthorne 1983), the scattering at $M(1)$ and $M(2)$ was represented as Nb and Ta, and the occupancies were refined independently. The refined scattering-values at the M sites were found to be equal.

Attempts to refine the structure in space groups $C2$ and Cc produced slightly lower R_1 indices but gave non-positive values for displacement parameters of O atoms. We tested for pseudomerohedral twinning, as β is close to 90° . Application of the twin matrix $1100/0\bar{1}0/0011$ (*i.e.*, 180° rotation around the a axis) gave a refined volume for a second individual of $0.095(2)$. Refined coordinates and anisotropic-displacement parameters of atoms are listed in Table 4, and selected interatomic distances are given in Table 5. Bond valences (Table 6) were calculated assuming that Nb, Ta, Ti and W are disordered over the $M(1)$ and $M(2)$ sites and occur in the proportions concordant with the bulk composition (Table 1). A table of structure factors and a cif file are available from the Depository of Unpublished Data on the Mineralogical Association of Canada website [document Billwiseite CM50_805].

CRYSTAL STRUCTURE

Coordination of cations

There are two M sites occupied by Nb, Ta, Ti and W, and octahedrally coordinated by O anions with

$\langle M-O \rangle$ distances of 1.968 and 1.976 Å, respectively. The refined site-scattering values (Hawthorne *et al.* 1995) show no indication of any order of cations over the two M sites [60.3(7) and 61.0(7) eps (electrons per site), respectively]. There are three Sb sites that the unit formula and site scattering indicate are occupied by Sb^{3+} with coordination numbers [6], [5] and [5], respectively. Inspection of Table 5 shows that all three Sb sites have three or four short bonds (<2.3 Å) and two long bonds (>2.3 Å). As shown in Figure 4, the shorter bonds occur on one side of the central cation, and the longer bonds occur on the opposite side. This arrangement is typical of lone-pair stereoactive cations where the lone pair of

electrons projects out on the side of the cation where the longer bonds occur (*i.e.*, where there is space to accommodate the lone pair).

The bond-valence sums at the $M(1)$ and $M(2)$ sites (Table 6) are in accord with the aggregate formal charge of the cations assigned to these sites in the chemical formula (Table 1). There are two [2]-coordinated anions, $\text{O}(3)$ and $\text{O}(8)$, and these each show one very strong bond to the cations at the M sites: 1.22 and 1.21 vu , respectively. All other anions are [3]-coordinated; there is a considerable range in the individual bond-valences (Table 6) related to the stereoactive lone-pair behavior of Sb^{3+} and the high degree of bond-length variation in

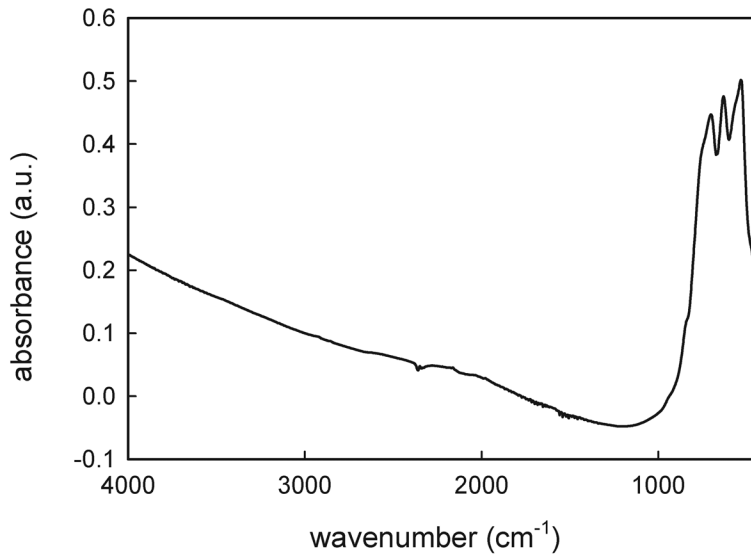


FIG. 3. The infrared spectrum of billwiseite.

TABLE 4. POSITIONS AND ANISOTROPIC-DISPLACEMENT PARAMETERS (\AA^2) OF ATOMS IN BILLWISEITE

Atom	x	y	z	U_{11}	U_{22}	U_{33}	U_{23}	U_{13}	U_{12}	U_{eq}
$M(1)$	0.05480(1)	0.25442(14)	1.13172(11)	0.0060(3)	0.0074(3)	0.0116(3)	-0.0003(2)	0.0003(2)	-0.0006(2)	0.0084(2)
$M(2)$	0.16463(1)	0.23919(15)	0.37332(15)	0.0062(3)	0.0069(3)	0.0093(3)	0.0003(2)	-0.00038(19)	0.0007(2)	0.0075(2)
$Sb(1)$	0	0.1983(3)	¾	0.0115(6)	0.0087(6)	0.0214(7)	0	0.0062(4)	0	0.0139(4)
$Sb(2)$	0.22152(2)	-0.20656(18)	0.32554(16)	0.0161(4)	0.0103(4)	0.0133(5)	-0.0012(3)	0.0035(3)	-0.0056(3)	0.0132(3)
$Sb(3)$	0.10997(2)	0.29999(19)	0.72606(17)	0.0126(4)	0.0096(5)	0.0163(5)	0.0014(3)	-0.0049(3)	-0.0035(3)	0.0129(3)
$O(1)$	0.12890(15)	0.413(2)	0.4089(18)	0.002(3)	0.013(4)	0.020(5)	0.001(4)	-0.002(3)	0.001(3)	0.012(2)
$O(2)$	0.02086(16)	0.087(2)	1.0867(18)	0.005(4)	0.014(4)	0.015(5)	-0.002(3)	-0.002(3)	-0.002(3)	0.011(2)
$O(3)$	0.06472(16)	0.013(2)	1.3665(18)	0.008(4)	0.013(4)	0.017(5)	0.010(4)	0.002(3)	0.000(3)	0.013(2)
$O(4)$	0.23860(15)	0.068(2)	0.1263(17)	0.005(4)	0.017(5)	0.013(4)	0.001(4)	-0.004(3)	-0.006(3)	0.012(2)
$O(5)$	0.08747(15)	0.4130(19)	1.0794(17)	0.006(4)	0.008(4)	0.015(4)	0.002(3)	0.002(3)	-0.005(3)	0.010(2)
$O(6)$	0.15095(16)	0.0356(19)	0.6676(18)	0.011(4)	0.006(4)	0.017(5)	0.002(3)	-0.003(3)	0.000(3)	0.011(2)
$O(7)$	0.19594(17)	0.085(2)	0.4244(18)	0.012(4)	0.012(4)	0.015(5)	-0.002(3)	0.001(3)	0.001(3)	0.013(2)
$O(8)$	0.17287(17)	0.521(2)	0.6311(19)	0.012(4)	0.016(5)	0.020(5)	-0.006(4)	-0.002(4)	0.000(4)	0.016(2)
$O(9)$	0.04268(16)	0.477(2)	0.8372(18)	0.008(4)	0.017(5)	0.015(5)	0.007(4)	-0.002(3)	0.002(4)	0.013(2)

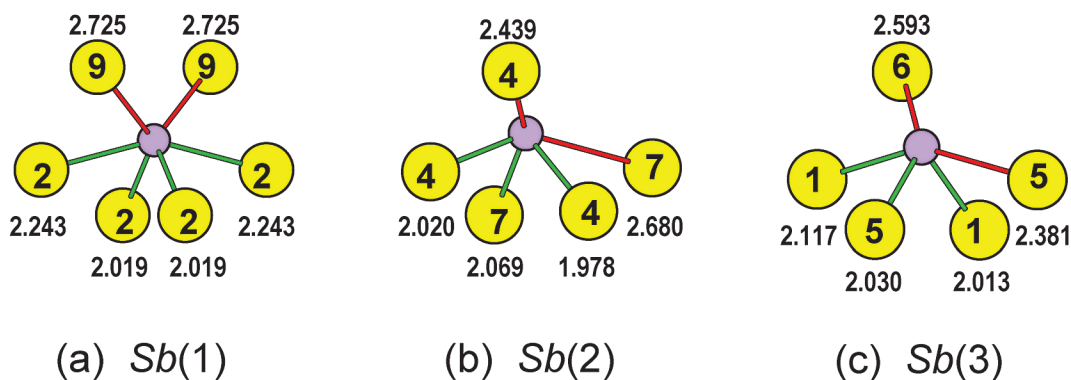


FIG. 4. The coordination around the Sb polyhedra in billwiseite; (a) $Sb(1)$; (b) $Sb(2)$ and (c) $Sb(3)$. Mauve circles: Sb^{3+} cations, yellow circles: anions; the numbers indicate the anion numbers in Table 5. Interatomic distances are shown in Å, green bonds are shorter than 2.3 Å, and red bonds are longer than 2.3 Å.

TABLE 5. SELECTED INTERATOMIC DISTANCES (Å) IN BILLWISEITE

$M(1)-O(2)$	2.026(10)	$M(2)-O(1)$	2.125(9)
$M(1)-O(3)$	1.840(10)	$M(2)-O(6)$	2.057(10)
$M(1)-O(3)a$	2.047(9)	$M(2)-O(6)a$	1.914(9)
$M(1)-O(5)$	1.956(8)	$M(2)-O(7)$	1.876(10)
$M(1)-O(9)b$	2.068(9)	$M(2)-O(8)$	2.026(9)
$M(1)-O(9)c$	1.868(10)	$M(2)-O(8)c$	1.844(10)
$<M(1)-O>$	1.968	$<M(2)-O>$	1.974
$Sb(1)-O(2)d,e$	2.019(10) $\times 2$	$Sb(2)-O(4)$	1.978(9)
$Sb(1)-O(2)f,g$	2.243(10) $\times 2$	$Sb(2)-O(4)e$	2.020(9)
$Sb(1)-O(9),h$	2.725(11) $\times 2$	$Sb(2)-O(7)$	2.069(10)
$Sb(2)-O(1)j$		$Sb(2)-O(4)i$	2.439(8)
$Sb(3)-O(1)$	2.013(9)	$Sb(2)-O(7)a$	2.680(10)
$Sb(3)-O(1)$	2.117(10)		
$Sb(3)-O(5)j$	2.030(9)		
$Sb(3)-O(5)f$	2.381(9)		
$Sb(3)-O(6)$	2.593(10)		

a: $x, \bar{y}, z - \frac{1}{2}$; b: $x, y, z - 1$; c: $x, \bar{y} + 1, z - \frac{1}{2}$; d: $\bar{x}, \bar{y}, z + 1$; e: $x, \bar{y}, z + \frac{1}{2}$; f: $x, y, z + 1$; g: $\bar{x}, y, \bar{z} + \frac{1}{2}$; h: $\bar{x}, y, \bar{z} + \frac{1}{2}$; i: $x, y - \frac{1}{2}, \bar{z} + \frac{1}{2}$; j: $x, \bar{y} + 1, z + \frac{1}{2}$.

the M polyhedra induced by the presence of [2]-coordinated anions in the structure. The cooperative distribution of strong and weak bonds leads to close adherence to the valence-sum rule of bond-valence theory.

Bond topology

The $M(1)$ octahedra share corners to form an open sheet parallel to (100) (Fig. 5a), as do the $M(2)$ octahedra (Fig. 5b), and the octahedra occupy the vertices of a 4^4 plane net. The [6]-coordinated $Sb(1)$ polyhedra link by sharing edges to form staggered chains that extend in the c direction (Fig. 5c). The $Sb(1)$ chains fit together in the b direction to form a discontinuous layer parallel to (100). The [5]-coordinated $Sb(2)$ polyhedra link by sharing edges to form staggered chains that extend in the c direction (Fig. 5e), but unlike the $Sb(1)$ and $Sb(3)$ chains, the $Sb(2)$ chains link in the b direction at two adjacent levels to form a continuous double sheet.

TABLE 6. BOND-VALENCE (vu) SUMMATIONS* FOR BILLWISEITE

	$M(1)$	$M(2)$	$Sb(1)$	$Sb(2)$	$Sb(3)$	Σ
$O(1)$		0.56			0.90 0.68	2.14
$O(2)$	0.74		0.88 ^{x2↓} 0.48 ^{x2↓}			2.10
$O(3)$	1.22 0.69					1.91
$O(4)$			0.99 0.88 0.28			2.15
$O(5)$	0.89				0.86 0.33	2.08
$O(6)$		0.68 1.00			0.19	1.87
$O(7)$		1.10		0.77 0.15		2.02
$O(8)$		0.74 1.21				1.95
$O(9)$	0.66 1.13		0.13 ^{x2↓}			1.92
Σ	5.33	5.29	2.98	3.07	2.96	
Ideal	5.27	5.27	3.00	3.00	3.00	

* Calculated with the parameters of Brown & Altermatt (1985).

the c direction (Fig. 5d), and as with the $Sb(1)$ chains, the $Sb(3)$ chains fit together in the b direction to form a discontinuous layer parallel to (100). The [5]-coordinated $Sb(2)$ polyhedra link by sharing edges to form staggered chains that extend in the c direction (Fig. 5e), but unlike the $Sb(1)$ and $Sb(3)$ chains, the $Sb(2)$ chains link in the b direction at two adjacent levels to form a continuous double sheet.

The M and Sb alternate along a in the following sequence (Fig. 6a): $M(1)-Sb(1)-M(1)-Sb(3)-M(2)-Sb(2)-Sb(2)-M(2)-Sb(3)$. The resulting structure

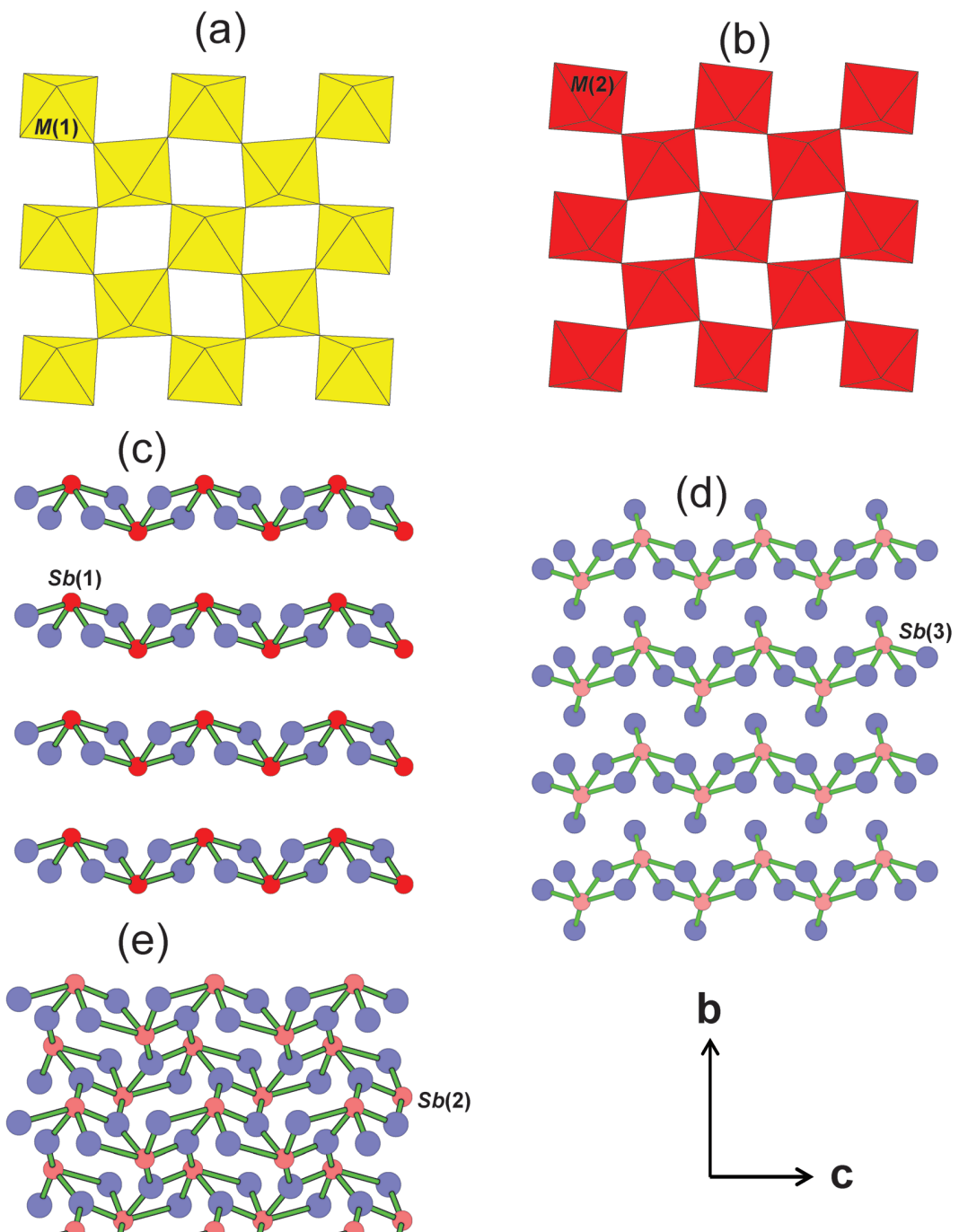


FIG. 5. The layers of polyhedra in the crystal structure of billwiseite projected onto (100). (a) The $[MO_4]$ sheet of corner-linked $M(1)$ octahedra (yellow); (b) the $[MO_4]$ sheet of corner-linked $M(2)$ octahedra (red); (c) the layer of chains of $Sb(1)$ polyhedra (Sb = red, O = blue); (d) the layer of chains of $Sb(3)$ polyhedra; (e) the sheet of $Sb(2)$ polyhedra.

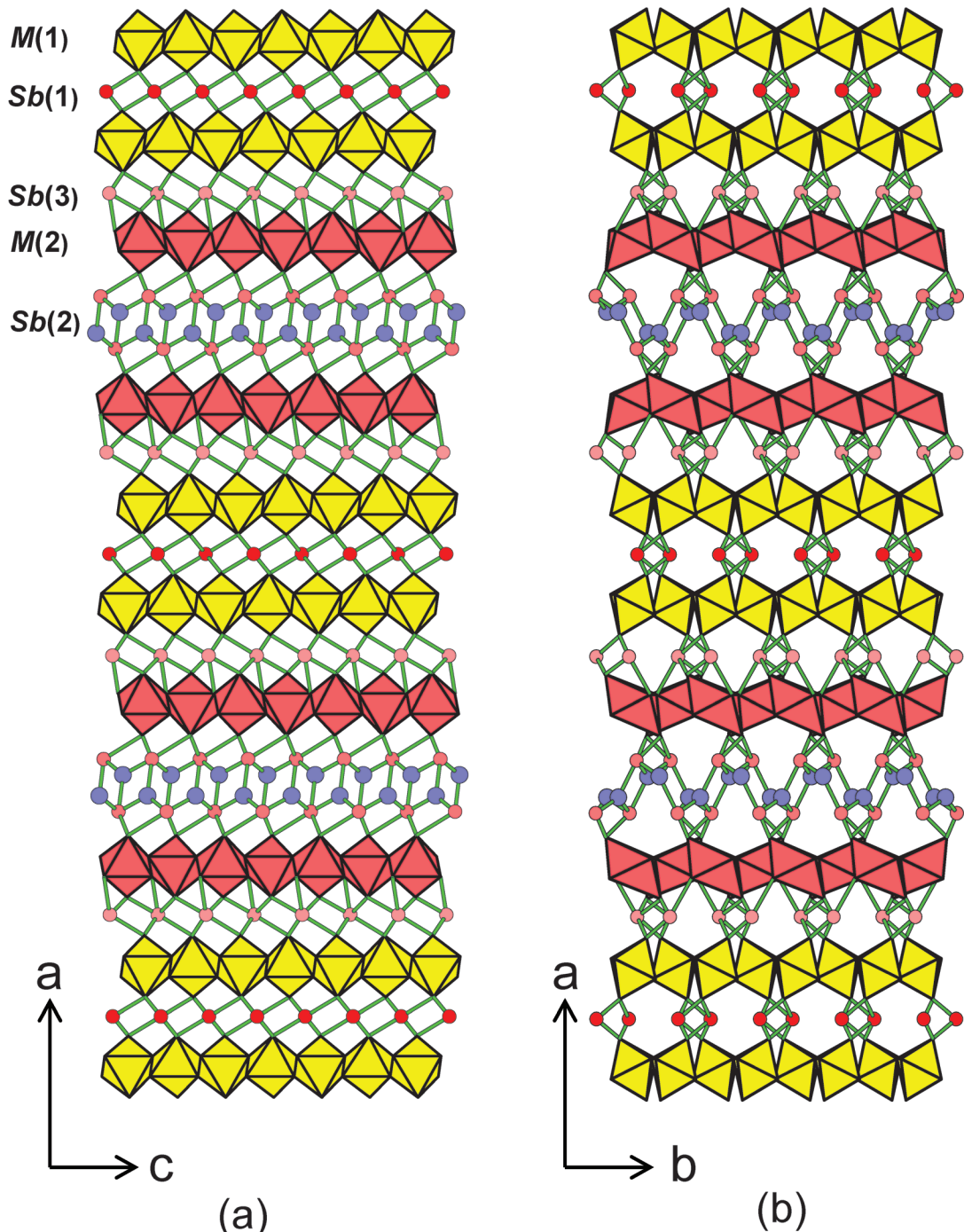


FIG. 6. The crystal structure of billwiseite (a) projected onto (010), showing the stacking of the *M* and *Sb* sheets, and (b) projected onto (001), showing the stacking of the *M* and *Sb* sheets.

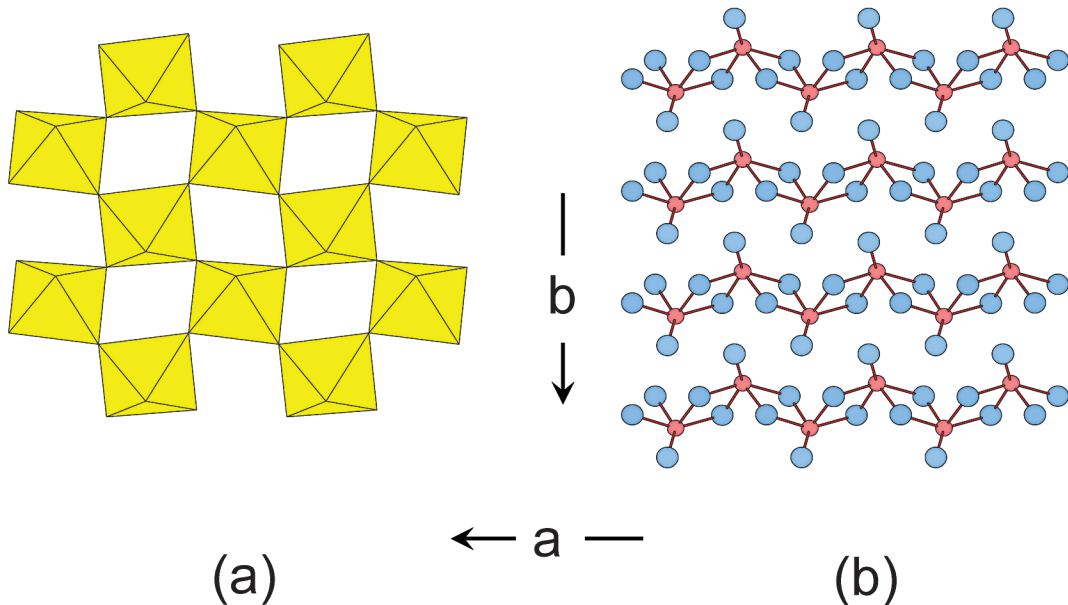


FIG. 7. The structural elements in the stibiotantalite structure. (a) The $[MO_4]$ sheet of corner-linked M (Ta,Nb) octahedra (yellow), and (b) the layer of chains of Sb polyhedra. Legend as in Figure 5.

is a framework of (Nb,Ta,W)-O octahedra and Sb^{3+} -O polyhedra (Fig. 6b) in which there is disorder of Nb, Ta, and W over the distinct octahedra in the structure.

Related structures

Billwiseite is not isostructural with any other mineral, but some of the features of the structural unit occur in other structures. The $M(1)$ and $M(2)$ sheets of octahedra in billwiseite (Figs. 5a, 5b) are similar to the (Nb,Ta) sheet of octahedra in stibiocolumbite (Zubkova *et al.* 2002) and stibiotantalite (Fig. 7a). The $Sb(3)$ layer in billwiseite (Fig. 5d) is similar to the Sb layer in stibiocolumbite and stibiotantalite (Fig. 7b). If we take into account the similarity of the $Sb(1)$ and $Sb(3)$ layers in billwiseite, we may consider the structure of billwiseite as slabs of the stibiotantalite structure separated by the $Sb(2)$ sheet (which is the only continuous Sb sheet in these structures).

RELATED MINERALS

With a metal:oxygen ratio of 1:2.22, billwiseite is a member of group 4D, metal:oxygen = 1:2 (and similar) in the classification of Strunz & Nickel (2001). It is in Class 8, multiple oxides containing niobium, tantalum and titanium of the Dana classification of Gaines *et al.* (1997). Data for related species are given in Table 7.

ACKNOWLEDGEMENTS

We thank Luca Bindi, Tony Kampf, Associate Editor Miguel Galliski and THE Editor, Bob Martin, for their comments on this paper. Initial analysis of the mineral was done in the electron-microprobe lab at Oregon State University, Corvallis, under the supervision of John Dilles and Roger Nielsen. This work was supported by a Canada Research Chair in Crystallography and Mineralogy and by Natural Sciences and Engineering Research Council of Canada Discovery, Equipment and Major Installation grants of the Natural Sciences and Engineering Research Council of Canada, and by Innovation grants from the Canada Foundation for Innovation to FCH. FC thanks the Dipartimento di Scienze della Terra e dell'Ambiente of the University of Pavia (Italy) where the diffraction data were collected.

REFERENCES

- BROWN, I.D. & ALTERMATT, D. (1985): Bond-valence parameters obtained from a systematic analysis of the inorganic crystal structure database. *Acta Crystallogr.* **B41**, 244-247.
- ČERNÝ, P. & ERCIT, T.S. (2005): The classification of granitic pegmatites revisited. *Can. Mineral.* **43**, 2005-2026.

TABLE 7. BILLWISEITE AND RELATED MINERALS

	Stibiotantalite	Stibiocolumbite	Tungstibite	Qitianlingite	Koragoite	Billwiseite
Formula	SbTaO_4	SbNbO_4	Sb_2WO_4	$\text{Fe}_2(\text{Nb,Ta})_2\text{WO}_{10}$	$\text{MnNb}_2(\text{Nb,Ta})_3\text{W}_2\text{O}_{20}$	$\text{Sb}_5\text{Nb}_3\text{WO}_{18}$
Symmetry	Orthorhombic	Orthorhombic	Orthorhombic	Orthorhombic	Monoclinic	Monoclinic
Space group	$Pc2,n$	$Pc2,n$	$P22_1$	$Pbcn$	$P2_1$	$C2/c$
a (Å)	4.911	4.929	8.59(2)	23.706(7)	24.73(2)	54.116(5)
b	11.814	11.797	9.58(2)	5.723(2)	5.056(3)	4.9143(5)
c	5.535	5.559	6.12(2)	5.045(3)	5.760(3)	5.5482(5)
β (°)	90	90	90	90	103.50(7)	90.425(2)
Z	4	4	4	4	2	4
$D_g \text{ cm}^{-3}$	7.53	5.68	6.69	6.30	6.11	6.33
Color	Shades of brown	Shades of brown	Dark green	Black	Black	Pale yellow
Cleavage	{001} distinct {100} indistinct	{001} distinct {100} indistinct	{001} perfect	{100} distinct	---	---
Hardness	5.5	5.5	~2	---	4–5	5
Occurrence	Pegmatite	Pegmatite	Fluorite deposit	Pegmatite	Pegmatite	Pegmatite

GAINES, R.V., SKINNER, H.C.W., FOORD, E.E., MASON, B. & ROSENSTEIG, A. (1997): *Dana's New Mineralogy* (eighth ed.). John Wiley and Sons, New York, N.Y.

HAWTHORNE, F.C. (1983): Quantitative characterization of site-occupancies in minerals. *Am. Mineral.* **68**, 287–306.

HAWTHORNE, F.C., UNGARETTI, L. & OBERTI, R. (1995): Site populations in minerals: terminology and presentation of results of crystal-structure refinement. *Can. Mineral.* **33**, 907–911.

LAURS, B.M., DILLES, J.H., WAIRRACH, Y., KAUSAR, A.B. & SNEE, L.W. (1998): Geologic setting and petrogenesis of symmetrically zoned, miarolitic granitic pegmatites at Stak Nala, Nanga Parbat – Haramosh massif, northern Pakistan. *Can. Mineral.* **36**, 1–47.

MADIN, I.P. (1986): *Structure and Neotectonics of the Northwestern Nanga Parbat – Haramosh Massif*. M.S. thesis, Oregon State University, Corvallis, Oregon.

POUCHOU, J.L. & PICOIR, F. (1985): 'PAP' $\phi(pZ)$ procedure for improved quantitative microanalysis. *In Microbeam*

Analysis (J.T. Armstrong, ed.). San Francisco Press, San Francisco, California (104–106).

SHEDDRICK, G.M. (2008): A short history of SHELX. *Acta Crystallogr. A* **64**, 112–122.

STRUNZ, H. & NICKEL, E.H. (2001): *Strunz Mineralogical Tables* (ninth ed.). Schweizerbart'sche Verlagsbuchhandlung, Stuttgart, Germany.

ZUBKOVA, N.V., PUSHCHAROVSKII, D.YU., GIESTER, G., SMO-LIN, A.S., TILLMANNS, E., BRANDSTÄTTER, F., HAMMER, V., PERETYAZHKO, I.S., SAPOZHNIKOV, A.N. & KASHAEV, A.A. (2002): Bismutocolumbite, $\text{Bi}(\text{Nb}_{0.79}\text{Ta}_{0.21})\text{O}_4$, stibiocolumbite, $\text{Sb}(\text{Nb}_{0.67}\text{Ta}_{0.33})\text{O}_4$, and their structural relation to the other ABO_4 minerals with stibiotantalite (SbTaO_4) structure. *Neues Jahrb. Mineral., Monatsh.*, 145–159.

Received July 26, 2011, revised manuscript accepted June 9, 2012.